Estuarine, Coastal and Shelf Science 323 (2025) 109427

Contents lists available at ScienceDirect

Estuarine, Coastal and Shelf Science

journal homepage: www.elsevier.com/locate/ecss

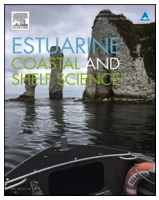

Seasonality and local nutrient loading drive changes in organic carbon in seagrass ecosystems in Hong Kong

Amrit Kumar Mishra [a], Katie M. Watson [a], Ho Tun Ng [a], Man Zhao [a], Chanaka Isuranga Premarathne Maha Ranvilage [a], Dwi Wai Shan Jaimie [a], Tse Cham Man [a], Christelle Not [a,b], Benoit Thibodeau [c], Juan C. Astudillo [d], Juan Diego Gaitán-Espitia [a,e,*]

[a] The Swire Institute of Marine Sciences and the School of Biological Sciences, The University of Hong Kong, Hong Kong SAR
[b] Department of Earth Sciences, The University of Hong Kong SAR, Hong Kong SAR
[c] Department of Earth and Environmental Sciences, School of Life Sciences, Chinese University of Hong Kong, Hong Kong SAR
[d] School of Science and Technology, Hong Kong Metropolitan University, Hong Kong SAR
[e] Institute for Climate and Carbon Neutrality, The University of Hong Kong, Hong Kong SAR

ARTICLE INFO

Keywords:
Eutrophication
Nitrogen pollution
Blue carbon
Soil organic carbon
Seagrasses
Urbanization

ABSTRACT

Natural variation in environmental conditions (e.g., seasonality) modulates the ecological dynamics and functioning of seagrass ecosystems. However, these characteristics can be altered by anthropogenic-driven pressures resulting from coastal urbanization (e.g., nutrient pollution), with significant effects on ecosystem service provision, including carbon sequestration and storage. Understanding these effects is complex as seagrasses exhibit different sensitives to environmental stress and change, generating species-specific responses that vary through temporal and spatial scales. Here, we tested this hypothesis by quantifying the seasonal variation in total carbon (C%; upper sediment layer, 15 cm), total nitrogen (N%), and stable isotopes ($\delta^{13}C$ and $\delta^{15}N$) in two seagrass species (i.e., *Halophila ovalis* and *H. beccarii*) in Hong Kong, one of the most urbanized coastal areas globally. The C:N ratios and $\delta^{15}N$ values indicated seasonal differences in local nitrogen source and accumulation, resulting in increased total seagrass biomass in the wet season. Isotope results suggested belowground seagrass tissues significantly contributed towards sediment carbon, particularly in the wet season, characterized by increased nitrogen loading.

1. Introduction

Seagrass ecosystems globally play an important role in carbon cycling, acting as natural carbon sinks (do Amaral Camara Lima et al., 2023). Modulated by their photosynthetic activity, seagrasses have a high capacity to sequester carbon dioxide from the atmosphere and seawater and storing it as autochthonous sedimentary organic carbon stocks (C_{stocks}) (Macreadie et al., 2021; Trevathan-Tackett et al., 2015). By using their canopies to filter fine particles transported by water as suspended matter, seagrasses can also capture organic carbon from allochthonous sources enhancing their sedimentary C_{stocks} (Barcelona et al., 2021; Nordlund et al., 2016; Rahayu et al., 2023). However, this carbon sequestration and storage capacity of seagrasses vary across temporal (e.g., seasons) and spatial (e.g., regions/latitude) scales, driven by local environmental conditions, as well as the ecological dynamics of seagrass populations and species (Egea et al., 2023a; Johannessen, 2022).

There is potential for these "blue carbon" ecosystems to serve as nature-based solutions (NbS) for carbon dioxide (CO_2) offsets in nationally determined contributions as part of climate change mitigation plans (Chausson et al., 2020; Stankovic et al., 2021). To achieve this, it is important to develop context-specific assessments to identify and predict the current and future carbon sink capacity of seagrass ecosystems over spatiotemporal scales (Johannessen, 2022; Gao et al., 2022; Ward et al., 2021). This is particularly relevant in areas where seagrasses are vulnerable to intense habitat modification (e.g., land reclamation), and the influence of other anthropogenic pressures from terrestrial and marine systems (Unsworth et al., 2019). Such losses can ultimately lead to shifts in seagrass distribution and metabolism, reducing net autochthonous organic carbon sequestration capacity (Mazarrasa et al., 2018),

This article is part of a special issue entitled: Blue CARE published in Estuarine, Coastal and Shelf Science.

* Corresponding author. The Swire Institute of Marine Sciences and the School of Biological Sciences, The University of Hong Kong, Hong Kong SAR.
E-mail address: juadiegaitan@gmail.com (J.D. Gaitán-Espitia).

https://doi.org/10.1016/j.ecss.2025.109427
Received 25 April 2025; Received in revised form 11 June 2025; Accepted 2 July 2025
Available online 5 July 2025

and potentially the release of blue carbon back into the atmosphere (Salinas et al., 2020; Serrano et al., 2020). As seagrasses are among the most threatened ecosystems globally, estimated to be declining at 0.9 % year^{-1} (Adams et al., 2020; Jiang et al., 2020; Luo et al., 2022), the remineralization of buried C_{stocks} represents a major concern in blue carbon and climate change science (Macreadie et al., 2019). Consequently, there has been increasing global attention to safeguard seagrasses and their role as NbS, protecting their blue carbon storage capacity (Christianson et al., 2022; United Nations Environment Programme, 2020).

Coastal nutrient loading represents a major threat to seagrass meadows, impacting their spatial dynamics (e.g., meadow migration/expansion), resulting in habitat fragmentation and degradation (Wang et al., 2022). Nutrient loading also alters seagrass ecosystems through several mechanisms (Burkholder et al., 2007), such as the alteration of sediment biogeochemistry (e.g., silt content), the reduction of functional traits (e.g., lower species diversity), the decline of productivity from increased carbon demand for additional ammonium assimilation (Egea et al., 2020), and the modification of ecological interactions (e.g., host-microbiota symbiosis (Yamuza-Magdaleno et al., 2024)), including increasing competition with micro/macroalgae for nutrient sources (Zribi et al., 2023). Therefore, eutrophication due to nutrient loading, can reduce the long-term carbon storage capacity in seagrass sediments (Burkholder et al., 2007). Such negative effects can be exacerbated by the interactive influence of high seasonal temperatures (e.g., in summer), which impacts seagrass carbon metabolism and accelerates the decomposition of labile carbon (Luo et al., 2022; Dahl et al., 2020; Pazzaglia et al., 2020; Soissons et al., 2018; Zhang et al., 2022). In recent years, there has been extensive research regarding seagrasses as blue carbon stocks, yet the influence of nutrient loading and seasonal variability at regional scales is still inadequately understood (Dencer-Brown et al., 2022; Duarte de Paula Costa and Macreadie, 2022). Regional scale assessments of blue carbon stocks are crucial to generate robust information to incorporate blue carbon ecosystems in national greenhouse gas inventories across International Panel for Climate Change (IPCC) tiers (i.e., Tier 1, 2 and 3), and for management pathways to be able to access carbon credit schemes (Howard et al., 2014).

In Hong Kong (SAR, China), one of the most urbanized coastal areas globally, seagrass ecosystems are represented by five species (*Halophila ovalis*, *Halophila minor*, *Halophila beccarii*, *Zostera japonica* and *Ruppia maritima*) (Shi et al., 2010). Except *R. maritima*, seagrasses are found in the shallow intertidal zone, associated with mangroves and saltmarshes (Archana et al., 2018). Despite their ecological importance, the effect of anthropogenic impacts (e.g., nutrient enrichment from riverine inputs, land runoff, wastewater disposal and aquaculture waste; see Table 1 in Archana et al. (2018)) on the dominant species (*H. ovalis* and *H. beccarii*), and the ecosystem services they provide (e.g., organic carbon storage), remain largely unexplored. In China, these two seagrasses have shown organic carbon storage capacity (*H. ovalis*: 7.14–12.26 Mg C ha^{-1}; *H. beccarii*: 4.21–20.05 Mg C ha^{-1} (Zhang et al., 2022; Huang et al., 2015; Jiang et al., 2017a), highlighting their potential utilization as NbS towards climate change mitigation (Meng et al., 2019). This organic carbon storage capacity, however, has been shown to decline in response to eutrophication (i.e., nitrogen enrichment (Zhang et al., 2022)), due to the intensification of anthropogenic activities along China's coastline (Wang et al., 2021; Ye et al., 2015). The effect of nutrient loading and subsequent reduction in organic carbon storage capacity has been observed for both *H. ovalis* (Jiang et al., 2019; Yang et al., 2018) and *H. beccarii* (Luo et al., 2022), particularly in China's south coast, where urbanization and aquaculture act as the main drivers (Wang et al., 2021).

Here, we aimed to i) quantify C_{stocks} of monospecific seagrass ecosystems in Hong Kong; ii) assess the effects of season (wet and dry) and anthropogenically driven (local nutrient input as a proxy of urbanization influence) influences on C_{stocks}; to ultimately iii) assess the NbS potential of these ecosystems towards Hong Kong's Climate Action Plan 2050 (Hong Kong SAR Government, 2021). We hypothesized that season, combined with local coastal nutrient enrichment, would positively influence the C_{stocks} of seagrass ecosystems in Hong Kong. To our knowledge, this study provides the first detailed quantification of seagrass species-specific C_{stocks} in Hong Kong, showcasing that the organic carbon storage capacity of these ecosystems can act as NbS for climate change mitigation and should be included in Hong Kong's nationally determined contributions under IPCC Tier 2 assessments (Howard et al., 2014).

2. Methods

2.1. Study area

Field surveys were conducted across four westerly sites in Hong Kong SAR (Pak Nai, Ha Pak Nai, San Tau, Yam O; Fig. 1). As part of the Greater Bay Area, these sites receive heavy sediment and nutrient loads from both the Pearl River (Zhu Jiang) and Shenzhen River (Sham Chun), with a salinity gradient southward along the westerly coastlines, producing estuarine conditions (Chen and Lee, 2022). During the wet season (summer), this natural stratification is particularly pronounced due to greater discharge from the Pearl River (Archana et al., 2018). Due to high local sediment and nutrient load (i.e., total nitrogen) and wastewater discharge, these sites are strongly influenced by high turbidity (~100–120 nephelometric turbidity units) (Archana et al., 2018; Environmental Protection Department, 2024). The two most widespread seagrasses in Hong Kong, yet still classified as regionally endangered, are the small herbaceous species *H. beccarii* (Ascherson, 1871) and *H. ovalis* ((R. Brown), J.D. Hooker, 1858). Both species can tolerate variable saline conditions and recover rapidly from anthropogenic disturbances due to their fast growth rate and ability to readily colonize intertidal areas on soft sand or mud substrates (Shi et al., 2010; Xuan et al., 2022).

2.2. Pak Nai and Ha Pak Nai

These sites are intertidal mudflats located ~1 km apart (Fig. 1), with mangrove stands and saltmarsh adjacent to *H. beccarii* meadows (Bass

Table 1
Physical parameters (mean ± SD) of the surface water over *Halophila ovalis* and *Halophila beccarii* meadows in Hong Kong during dry and wet seasons. Statistical significance ($p < 0.05$) between species and seasons were tested using two-way ANOVA, with season (wet and dry) and species (*H. ovalis* and *H. beccarii*) as fixed factors.

Parameters		Species		Two-way ANOVA results			
	Season	*H. ovalis*	*H. beccarii*	Variable	MS	F-value	*p*-value
pH	Dry	8.44 ± 0.47	8.56 ± 0.18	Species	0.14	$F_{(1,26)} = 0.61$	0.44
	Wet	9.31 ± 0.76	9.48 ± 0.49	Season	5.81	$F_{(1,26)} = 24.23$	**<0.0001**
Temp (°C)	Dry	21.74 ± 4.25	23.16 ± 3.73	Species	162.90	$F_{(1,34)} = 8.33$	**0.006**
	Wet	24.07 ± 4.49	31.23 ± 5.09	Season	238.90	$F_{(1,34)} = 12.23$	**0.001**
Salinity (PSU)	Dry	29.91 ± 4.46	17.87 ± 8.50	Species	342.90	$F_{(1,27)} = 7.86$	**0.009**
	Wet	14.00 ± 7.84	12.00 ± 6.41	Season	825.90	$F_{(1,27)} = 18.93$	**0.0002**

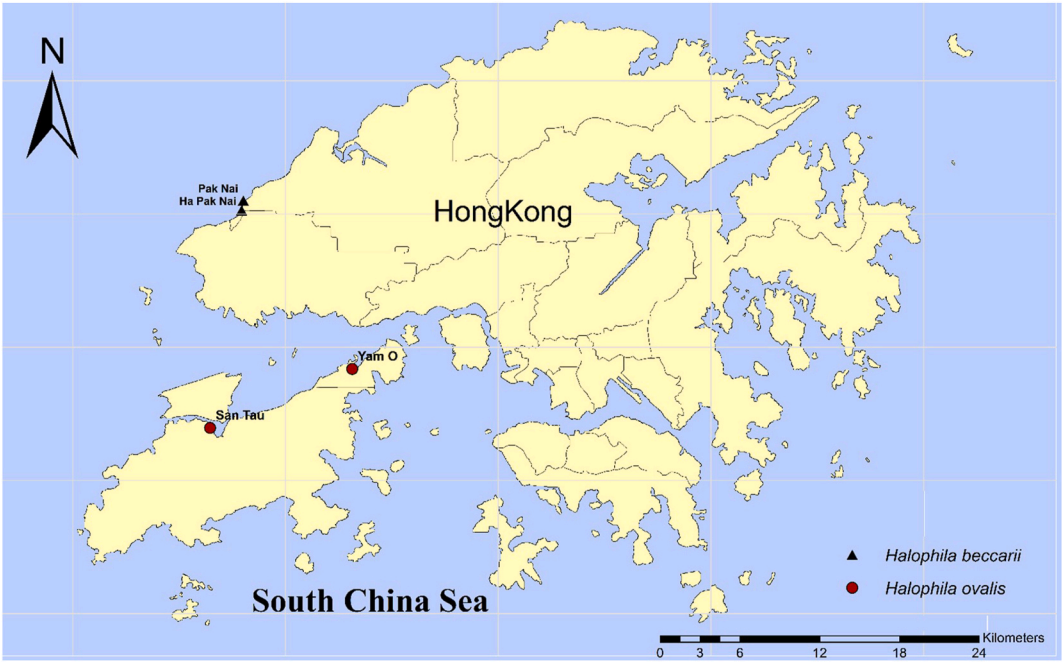

Fig. 1. Map showing the four study sites for *Halophila ovalis* and *Halophila beccarii* in Hong Kong.

and Falkenberg, 2023). Mangrove stands are characterized by *Sonneratia apetala, Acanthus ilicifolius* and *Kandelia obovata* (Morton, 2016), whereas saltmarsh species include *Sporobolus alterniflorus, Suaeda australis, Sesuvium portulacastrum, Sporobolus virginicus* and *Ipomoea pes-caprae* (A. Mishra, personal field observation, 2022). Mangrove and saltmarsh habitats are abundant towards the upper shore, with *H. beccarii* occupying the intertidal zone, and aquaculture oyster beds extending across the lower shore. These sites also provide crucial feeding and nesting habitat for the endangered Chinese horseshoe crab *Tachypleus tridentatus* (Tanacredi et al., 2009). The total area of the seagrass meadows in Pak Nai and Ha Pak Nai are ~3.80 ha and ~6.83 ha, respectively (Fong, 1998).

2.3. San Tau and Yam O, Lantau Island

These sites follow a similar ecosystem matrix as Pak Nai and Ha Pak Nai, with mangroves towards the upper shoreline, *H. ovalis* meadows in the muddy intertidal region covering ~4.90 ha, and oyster beds across the lower shore (Bass and Falkenberg, 2023). The mangroves in San Tau are inhabited by mixed stands of *K. obovata*, *Avicennia marina*, *Bruguiera gymnorrhiza*, *Excoecaria agallocha*, *Lumnitzera racemosa* and *Hibiscus tiliaceum* (Morton, 2016), with saltmarsh characterized by *S. portulacastrum*, *S. australis*, *S. virginicus* and *Limonium sinense* (A. Mishra, personal field observation, 2022). Yam O has a total seagrass area of ~0.87 ha with mangrove stands containing *K. obovata, A. marina*, *B. gymnorrhiza*, *H. tiliaceum*, and *Aegiceras corniculatum* in the upper intertidal zone (A. Mishra, personal field observation, 2022). In comparison to Pak Nai and Ha Pak Nai, there are no saltmarshes directly adjacent to *H. ovalis* meadows in San Tau or Yam O. Both sites are also more exposed to housing developments and land reclamation in nearby Lantau Island, in comparison to meadows in Pak Nai and Ha Pak Nai.

2.4. Seagrass and associated habitat biomass sampling

At each of the four sites, transects were conducted in the wet (summer; May–September) and dry season (winter; December–March) of 2021–2022. Triplicate measurements of physical parameters including temperature, salinity, and pH of the surface water above seagrass meadows were measured in the field using handheld multi-probes (Go Direct®- Vernier Probes, USA). Triplicate 50 m transect parallel to the beach was deployed, along which nine seagrass biomass cores (⌀ 6.5 cm) were collected at random to a depth of 10 cm. Biomass cores were capped and stored in an icebox for transportation to the University of Hong Kong (HKU) laboratory. Here, seagrass biomass was washed with distilled water to remove debris, then a glass slide was used to gently scrape away any epiphytic macroalgae on the seagrass leaves. Samples were separated into aboveground (leaf) and belowground (roots and rhizomes) biomass, placed into clean aluminum foil, and oven dried at 60 °C for 48 h. After drying, seagrass biomass was homogenized using a ball mill (Retsch, MM400, USA) and stored for further analysis. Similarly, leaves of mangrove and saltmarsh species (as above) were hand-picked during seagrass sampling, processed as described above and stored for further analysis (Howard et al., 2014).

2.5. Sediment sampling

Acrylic sediment corers (⌀ 5.5 cm) were used for each 50 m transect (n = 3 per transect) to collect sediment samples from each site, adjacent to the seagrass biomass cores. The sediment core depth was restricted to 15 cm, as both seagrass species are small and their influence on sediment organic carbon accumulation is restricted to upper sedimentary layers (Meng et al., 2019; Premarathne et al., 2021). After collection, sediment cores were capped and stored in an icebox for transportation to the HKU laboratory. At the laboratory, sediment cores were divided into 5 cm intervals (5, 10 and 15 cm), placed into clean aluminum foil, and oven dried at 60 °C for 48 h. After drying, each sample was weighed to calculate dry bulk density (DBD; g DW cm^{-3}), as described in Howard et al. (2014). The sediment carbon density (SCD; g cm^{-3}) was calculated by multiplying the DBD with sediment carbon content (%). Next, dried samples were individually homogenized using a ball mill (Retsch, MM400, USA) and stored for further analysis. From each homogenized sample, the organic matter content (OM%) of the sediment was estimated using the loss on ignition method, as presented below, whereby subsamples (5 g) were combusted at 500 °C for 4.5 h in a muffle furnace (Howard et al., 2014). The loss on ignition was calculated using equation (1):

$$\text{Loss on ignition } (\%) = \left[\frac{A-B}{A}\right] x\ 100 \quad \text{(Eq.1)}$$

Where A is the initial weight of the dried sediment (g), and B is the final weight of the sediment (g) after combustion.

Additionally, from each homogenized sample, a subsample (0.30 mg) was acidified (1 M HCl) to remove carbonates. After the addition of HCl, the subsamples were stored in a fume hood chamber until no further bubble formation was detected, then the subsamples were oven dried at 60 °C for 24 h.

2.6. Seagrass biomass and sediment analysis

Seagrass (aboveground and belowground), mangrove (aboveground) and saltmarsh biomass (aboveground), as well as sediment samples (acidified and non-acidified), were analyzed in duplicate for composition of carbon and nitrogen elemental concentrations and stable isotopes ($\delta^{13}C$ and $\delta^{15}N$) using a Flash Elemental Analyzer coupled to a DELTA V isotope ratio mass spectrometer (Eurovector, EA3028). Following in-house standards, acetanilide (iACET#1, $\delta^{13}C = -29.53$ ‰, $\delta^{15}N = 1.18$ ‰) was used for calibration and precision determination (0.2 ‰) with Vienna Peedee Belemnite and atmospheric air used as isotope references for carbon and nitrogen, respectively.

The IsoSource software (version 1.3.1 Environmental Protection Agency, USA) was used to estimate the feasible contributions of all carbon sources across seasons (Phillips et al., 2005). A mixing model approach was utilized to calculate the relative contributions of all carbon sources using all possible combinations of seagrass (aboveground and belowground), mangrove (aboveground), saltmarsh (aboveground) and sediment particulate organic matter (obtained from Fu et al. (2020)) (Phillips and Gregg, 2003). The model had two fixed parameters: the source increment was set at 1 % and the mass balance tolerance was set at 0.01 % (Zhang et al., 2020). The fixed mass balance tolerance ensured that the difference between the sum of the weighted isotopic values for each source and the acceptor isotopic values did not exceed 0.01 %.

2.7. Carbon stock calculations

The total biomass C_{stocks} (Mg C ha^{-1}) of both seagrass species were calculated following the Blue Carbon Manual standard methods (Howard et al., 2014). The total sediment C_{stocks} (Mg C ha^{-1}) were calculated by adding the total C_{stock} of each sediment core interval (5, 10, 15 cm). The mean seagrass ecosystem C_{stock} (Mg C ha^{-1}) were calculated by adding the mean seagrass aboveground biomass C_{stocks} to the mean belowground sediment C_{stocks}. This then allowed for the species-specific mean seagrass ecosystem C_{stocks} (Mg C) to be calculated by multiplying the total meadow area of each species with the mean ecosystem C_{stocks}. The CO_2 equivalent (Mg CO_2 ha^{-1}) was calculated by multiplying the CO_2 conversion factor (3.67) by the mean C_{stocks} of both seagrass species and upscaled to total meadow area (Howard et al., 2014).

2.8. GIS mapping of sediment and water column data

Geographic information system (GIS) techniques are now widely used in generating continuous spatial patterns of trace elements at regional scales (Sachithanandam et al., 2022; Gu et al., 2012). Here, we estimated the spatial distribution of physical parameters of the water column (i.e., pH, temperature, and salinity) and sediment variables (i.e., OM%, DBD, SCD, total carbon (C%) and total nitrogen (N%)) for both seasons based on the measured values using the Kriging interpolation method in ArcGIS (version 10.8). The Kriging approach uses the semi variogram to express spatial continuity (i.e., autocorrelation), and measures the strength of the statistical correlation as a function of distance (see (Cressie, 1988)). Despite the observations being spatially concentrated, the objective was to visualize the spatial distribution of physical parameters between seasons, in relation to seagrass distribution, in Hong Kong.

2.9. Social cost of carbon and CO_2 equivalent

The social cost of carbon indicates the economic cost associated with climate change-related damage (or benefit) caused by the emission of one ton of CO_2, or its equivalent (Nordhaus, 2017; Ricke et al., 2018). We utilized a regional approach to estimate the social cost of carbon, rather than a global approach, as country-level estimates promote a better understanding of regional impacts of carbon emissions, leading to improved adaptation and compensation measures (Ricke et al., 2018). The estimate of the social cost of carbon for China (inc. Hong Kong), was US$ 24 (HKD$ 186.48) per ton of CO_2 used (Ricke et al., 2018). A currency conversion of USD$ 1 = HKD$ 7.77 was used to estimate the price of CO_2 in HKD$.

2.10. Statistical analysis

A two-way ANOVA was used to determine the effect of sediment characteristics (dry bulk density (DBD, g cm^{-3}), sediment carbon density (SCD, g cm^{-3}), total carbon (C%) and nitrogen (N%), stable isotopes of carbon ($\delta^{13}C$ ‰) and nitrogen ($\delta^{15}N$ ‰), C_{stocks} (Mg C ha^{-1})), and seagrass (aboveground and belowground biomass) using seagrass species (*H. ovalis* and *H. beccarii*), and season (dry and wet) as fixed factors. Data was checked for normality and homogeneity of variance using a Shapiro-Wilk and Levene's test, respectively. As SCD did not meet the assumptions of normality, a $\log^{10}$ transformation was performed. In the case of significant interactions between factors, the Holm-Šídák test was performed for multiple comparisons of means. Next, we applied multivariate techniques to explore the correlation between physiochemical chemicals across seasons for each seagrass species in a continuous way. We used a principle component analysis (PCA) with the descriptors including surface water environmental parameters (pH, temperature, salinity), sediment organic matter (OM%), dry bulk density (DBD, g cm^{-3}), sediment total nitrogen (N%), sediment total carbon (C%) and seagrass (aboveground and belowground) biomass (g DW m^{-2}) in dry and wet seasons for *H. ovalis* and *H. beccarii*. A non-linear regression (second order polynomial (quadratic) curve fit was used to derive the relationship between N% in seagrass biomass and the log (Y) transformed C:N ratios to determine external nitrogen input into seagrass ecosystems (Duarte, 1990). All statistical tests were conducted at a significance level of $p < 0.05$ in GraphPad Prism software (version 10.3). Note that all results for core samples are given as the mean ± SD.

3. Results

3.1. Physicochemical parameters

Seasonality was found to strongly influence all surface water physical parameters (Table 1) above *H. ovalis* and *H. beccarii* seagrass meadows, with pH (ANOVA, $F_{1,26} = 24.23$, $p < 0.0001$) and temperature (ANOVA, $F_{1,34} = 12.23$, $p = 0.001$) being significantly higher in the wet season (Table S1; Fig. S1). Conversely, salinity was significantly lower in the wet season, compared to the dry season (ANOVA, $F_{1,27} = 18.93$, $p = 0.0002$; Table 1). Temperature was significantly higher in the surface water above *H. beccarii* meadows (ANOVA, $F_{1,34} = 8.33$, $p = 0.006$), whereas salinity was found to be significantly lower (ANOVA, $F_{1,27} = 7.86$, $p = 0.009$; Table 1).

3.2. Sediment variables

The mean sediment organic matter content was significantly different between seagrass species ($F_{1,20} = 7.98$, $p = 0.01$) and season ($F_{1,20} = 7.64$, $p = 0.01$; Fig. 2a; Table S2). The DBD was significantly different only across species ($F_{1,30} = 5.47$, $p = 0.02$), and SCD was

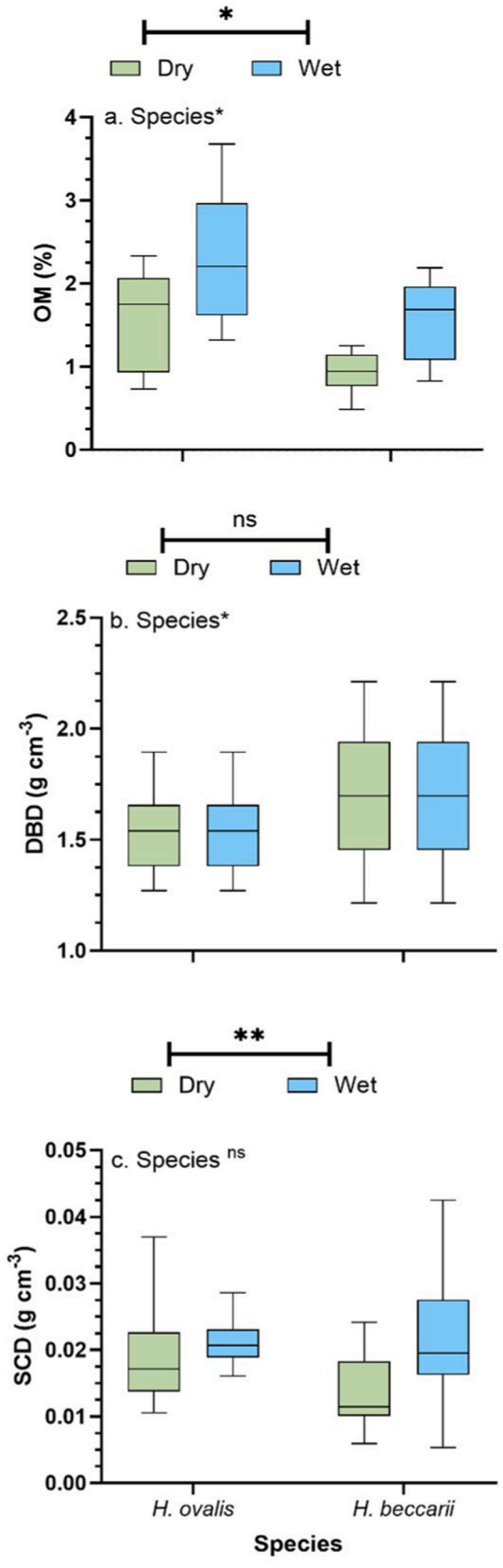

Fig. 2. Boxplots illustrating sediment a) organic matter (OM%), b) dry bulk density (DBD, g cm^{-3}), and c) sediment carbon density (SCD, g cm^{-3}) from cores taken from *Halophila ovalis* and *Halophila beccarii* meadows in dry and wet seasons in Hong Kong. Statistical significance ($p < 0.05$) was derived from a two-way ANOVA using season (dry and wet) and species (*H. ovalis* and *H. beccarii*) as fixed factors ($p < 0.001$**, $p < 0.05$*, not significant = ns).

significantly different only across seasons ($F_{1,30} = 11.33$, $p = 0.01$), respectively (Fig. 2; Table S2). The mean sediment organic matter content of *H. ovalis* (1.59 ± 0.60 %) and *H. beccarii* (0.93 ± 0.25 %) meadows were 1.4-fold and 1.7-fold lower than the sediment organic matter of both species (*H. ovalis*; 2.31 ± 0.87 %, *H. beccarii*; 1.57 ± 0.50 %) in the wet season respectively (Fig. 2a). The mean sediment DBD of *H. ovalis* meadows (1.54 ± 0.20 g DW cm^{-3}) was 1.1-fold lower than the sediment DBD of *H. beccarii* (1.70 ± 0.33 g DW cm^{-3}) meadows (Fig. 2b). The mean SCD of *H. ovalis* (0.019 ± 0.007 g C cm^{-3}) and *H. beccarii* (0.014 ± 0.005 g C cm^{-3}) in the dry season was 1-fold and 1.6-fold lower than the SCD of both species (*H. ovalis*; 0.021 ± 0.003 g C cm^{-3}, *H. beccarii*; 0.023 ± 0.01 g C cm^{-3}) in the wet season (Fig. 2c).

The seasonal relationships between water physical parameters and sediment variables with both seagrass traits are presented through PCA analysis (Fig. 3, Table S3). For *H. ovalis* in the dry season, PC1 (42.12 %) and PC2 (23.94 %) explained a cumulative variation of 66.05 %, whereas in wet season the PC1 (57.60 %) and PC2 (16.35 %) explained a cumulative variation of 73.95 % (Fig. 3a and b). For *H. beccarii* in dry season, the PC1 (37.09 %) and PC2 (20.45 %) explained a cumulative variation of 57.54 %, whereas in the wet season the PC1 (38.46 %) and PC2 (24.03 %) showed a cumulative variation of 62.49 % (Fig. 3c and d).

3.3. Seagrass biomass and sediment variables

Significant differences were observed between seasons ($F_{1,51} = 4.51$, $p < 0.0001$) and species ($F_{1,51} = 23.21$, $p = 0.02$) for the mean C% content in seagrass biomass (aboveground and belowground; Table S5). The C% content in *H. ovalis* biomass was 1.1-fold higher in both aboveground (31.67 ± 5.42 %) and belowground (27.88 ± 7.38 %) tissues in the dry season, compared to the wet season (Table S5). The C% content in *H. beccarii* biomass was also 1.4-fold higher in aboveground tissues (34.51 ± 4.14 %) in the dry season, but conversely, C% content in belowground tissues (32.99 ± 2.04 %) were found to be 1.1-fold higher in the wet season (Table S5). Significant differences were also observed between seasons ($F_{1,30} = 7.78$, $p = 0.0009$) and species ($F_{1,30} = 14.05$, $p = 0.0008$) for the mean C% content in sediment cores (Table S4). The sediment C% content in *H. ovalis* (1.36 ± 0.22 %) and *H. beccarii* (1.36 ± 0.22 %) meadows were 1-fold and 1.6-fold higher in the wet season, respectively (Table S4).

Seasonal differences of mean N% content in seagrass biomass were detected ($F_{1,85} = 46.71$, $p < 0.0001$; Table S5). The aboveground (2.48 ± 0.56 %) and belowground (1.91 ± 0.76 %) tissues of *H. ovalis* accumulated 1-fold and 2-fold more N% content in the wet season, respectively (Table S5). However, the aboveground tissues (3.70 ± 0.45 %) of *H. beccarii* accumulated 1.5-fold higher N% content in the dry season, whereas the belowground tissues accumulated 1.4-fold higher N% content in the wet season (2.75 ± 0.55 %; Table S5). The mean N% content in the sediment of *H. ovalis* meadows was 1-fold higher in the dry season (0.15 ± 0.04 %), whereas the sediment N% content in *H. beccarii* meadows was comparable between seasons (dry: 0.06 ± 0.07 %; wet: 0.09 ± 0.03; Table S4).

The $\delta^{13}C$ isotopic composition of the seagrass biomass varied significantly between seasons ($F_{1,81} = 13.15$, $p < 0.0001$) and species ($F_{1,61} = 6.10$, $p < 0.0001$; Table S5). The $\delta^{13}C$ values for aboveground biomass of *H. ovalis* (−16.48 ± 1.03 ‰) and *H. beccarii* (20.57 ± 0.62 ‰) were depleted in wet season, compared to the dry season (*H. ovalis*: −13.30 ± 0.97 ‰; *H. beccarii*: −15.91 ± 0.96 ‰; Table S5). Similarly, the $\delta^{13}C$ isotopic composition of the seagrass sediment also varied significantly between seasons ($F_{1,81} = 13.15$, $p < 0.0001$; Table S4).The sediment $\delta^{13}C$ values of *H. beccarii* (−25.16 ± 1.36 ‰ in dry season; −25.08 ± 1.30 ‰ in wet season) showed depleted composition compared to *H. ovalis* sediment (−22.48 ± 0.89 ‰ in dry season; −22.81 ± 1.16 ‰ in wet season; Table S4). The $\delta^{15}N$ isotopic composition in seagrass biomass also varied significantly between seasons ($F_{5,142} = 23.3$, $p < 0.0001$) and species ($F_{1,81} = 13.15$, $p = 0.01$; Table S5). The aboveground biomass of *H. ovalis* and *H. beccarii* both showed

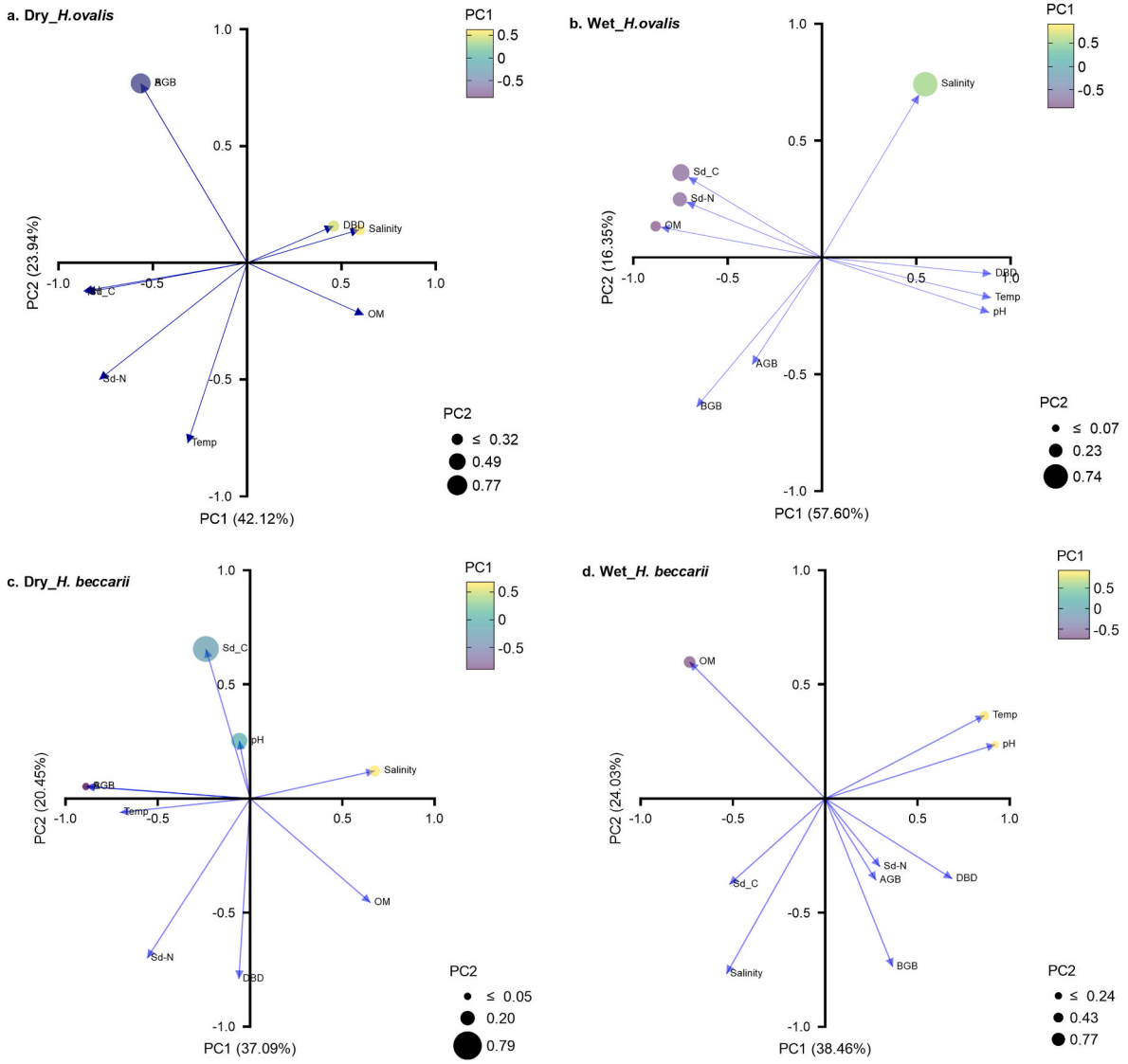

Fig. 3. Principal component analysis (PCA) loadings between environmental parameters of surface water (pH, temperature, salinity), sediment organic matter (OM %), dry bulk density (DBD, g cm^{-3}), sediment total nitrogen (N%), sediment total carbon (C%) and seagrass aboveground (AG) and belowground (BG) biomass (g DW m^{-2}) in dry and wet seasons for *H. ovalis* (a & b) and *H. beccarii* (c & d). The contribution of each variable to the PCA in both dry and wet seasons for both seagrass species is presented in Table S4.

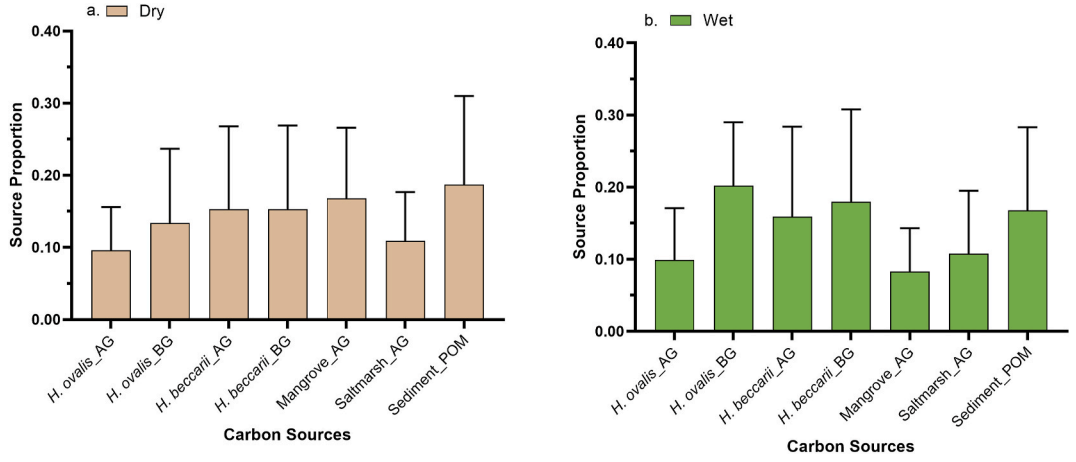

Fig. 4. Proportional source contributions to the sediment carbon pool (C%) in both *H. ovalis* and *H. beccarii* in the a) dry and b) wet season in Hong Kong respectively.

substantially enriched $\delta^{15}N$ in the wet season (11.22 ± 0.94 ‰; 9.32 ± 1.43 ‰), in comparison to the dry season (9.28 ± 0.80 ‰; 6.93 ± 5.12 ‰; Table S5). The seagrass sediment $\delta^{15}N$ isotopic composition also varied significantly between seasons ($F_{5,142} = 23.3$, $p = 0.02$) and species ($F_{1,81} = 13.15$, $p = 0.001$; Table S4). The seagrass sediment exhibited $\delta^{15}N$ enrichment in the wet and dry seasons, with depleted isotopic composition in the dry season for both species (*H. ovalis*: 6.12 ± 0.89 ‰, *H. beccarii* 6.59 ± 0.33 ‰) respectively (Table S4).

The mixing model of relative contributions of all carbon sources, showed that the belowground-tissue contribution of both *H. ovalis* (0.202 ± 0.088) and *H. beccarii* (0.180 ± 0.128) increased 1.5-fold and 1.2-fold in the wet season, respectively (Fig. 4; Table S6). The contribution from mangroves (aboveground; 0.083 ± 0.060) and sediment particulate organic matter (0.168 ± 0.115) decreased 2-fold and 1.1-fold in the wet season, respectively (Fig. 4; Table S6)., Whereas saltmarsh (aboveground) contributions remained comparable across seasons (0.109 ± 0.068 (dry) and 0.108 ± 0.087 (wet); Fig. 4; Table S6). The C:N ratios versus N% content in seagrass biomass and sediment of both species indicated external input of nitrogen during the wet season, and the subsequent accumulation of nitrogen into the seagrass biomass (Fig. 5; Fig. S3, Table S4; Table S5).

3.4. Seagrass biomass and sediment carbon stocks: the social cost

Seagrass biomass showed significant variation between species ($F_{1,46} = 14.44$, $p < 0.001$), but not between seasons (Fig. S5; Table S5). The total biomass (aboveground + belowground) of *H. ovalis* (24.93 ± 4.63 g DW m^{-2}) and *H. beccarii* (61.27 ± 16.98 g DW m^{-2}) was 1-fold and 1.6-fold higher in the wet season (Table S4). The sediment (upper 15 cm) C_{stocks} showed significant variation between seasons ($F_{1,20} = 6.05$, $p = 0.02$; Fig. 6b; Table S4). In the wet season, the sediment C_{stocks} in *H. ovalis* (31.44 ± 4.04 Mg C ha^{-1}) and *H. beccarii* (33.85 ± 11.34 Mg C ha^{-1}) meadows were 1-fold and 1.7-fold higher, respectively (Fig. 6b; Table S4).

The CO_2 equivalent of sediment carbon in *H. ovalis* (115.4 ± 14.81 Mg CO_2 ha^{-1}) and *H. beccarii* (124.26 ± 41.61 Mg CO_2 ha^{-1}) was 1-fold and 1.7-fold higher in wet season than dry season (Fig. 6d; Table S4). Between seasons (dry-wet), total C_{stocks} in *H. ovalis* biomass ranged between 0.076 and 0.071 Mg C ha^{-1}, whereas in *H. beccarii* C_{stocks} ranged between 0.12 and 1.15 Mg C ha^{-1} (Fig. 6; Table S4).

The contribution of sediment C_{stocks} (190.16 ± 81.67 Mg C) across both seasons was 99.9 % higher than *H. ovalis* biomass (0.54 ± 0.20 Mg C), with a CO_2 equivalent of 697.90 ± 299.73 Mg CO_2 and 1.99 ± 0.81 Mg CO_2, respectively (Table S4, Table S5). Similarly, the contribution of sediment C_{stocks} (285.68 ± 54.29 Mg C) was 99.9 % higher than *H. beccarii* biomass (1.56 ± 0.46 Mg C), with a CO_2 equivalent of 1048.47 ± 198.88 Mg CO_2 and 4.62 ± 1.15 Mg CO_2, respectively (Table S4, Table S5). The total CO_2 equivalent reduction potential across both seasons for *H. ovalis* meadows (San Tau + Yam O = 5.78 ha) is 348.92–350.97 Mg CO_2, and for *H. beccarii* meadows (Pak Nai + Ha Pak Nai = 10.63 ha) is 431.45–621.64 Mg CO_2. Therefore, the social cost of carbon of the CO_2 equivalent stored in the sediment of *H. ovalis* meadows is HK$ 0.12 ± 0.01 million (US$ 0.01 million), and in *H. beccarii* meadows is valued at HK$ 0.19 ± 0.07 million (US$ 0.02 million).

4. Discussion

The mean sediment C_{stocks} of *H. ovalis* (28.25–31.44 Mg C ha^{-1}; Fig. 6c) and *H. beccarii* (20.51–33.85 Mg C ha^{-1}; Fig. 6c) in the upper surface sediment (15 cm) were comparable with the mean sediment C_{stocks} reported for seagrass in Southeast Asia (14.51–37.65 Mg C ha^{-1} (Stankovic et al., 2021; Alongi, 2020)) and globally (17.25–124.35 Mg C ha^{-1} (Kennedy et al., 2010)). The mean sediment C_{stocks} in the study sites were multi-fold higher compared to sediment C_{stocks} reported for *H. ovalis* (6.5–12.5 Mg C ha^{-1}) and *H. beccarii* (4.5–11.3 Mg C ha^{-1}) meadows on the coast of Hainan Island, China (Jiang et al., 2017b), and *Halophila* spp. (0.01 0.03 Mg C ha^{-1}) meadows in Southern China (Ren et al., 2024). These earlier studies collected sediment samples from the top 5–10 cm (Jiang et al., 2017b) and 15 cm (Ren et al., 2024) sediment layers, a range that is comparable with the upper 15 cm sampled in monospecific meadows in this study. The seagrass meadows studied here are characterized by dynamic intertidal environments with high seasonal influences and variability in the inflow/outflow of organic matter into sediment and the subsequent loss/gain of C_{stocks} (Meng et al., 2019; Fu et al., 2021; Martins et al., 2022). In this study, the organic matter input into the sediments of both seagrass species was ~1.5-fold higher in the wet season, compared to dry season (Fig. 4). These seasonal differences are likely explained by greater anthropogenic and riverine inputs during the wet season, enabling seagrass meadows to filter fine particles from the water column to form muddy sediments (Su et al., 2020; Xu et al., 2008).

The wet season, combined with local anthropogenic and riverine nutrient loading, alters sediment organic matter content due to high turbidity and deposition of fine particles in seagrass meadows, thus positively influencing the sediment organic matter pool (Zhang et al., 2022; Zhou et al., 2011). From our results, this is clearly inferenced from the sediment organic matter of both seagrass species having a positive correlation with sediment nutrient (N%) content in the wet season, when organic matter inflow from both riverine and local land run-off sources is high (Fig. 5). These different sources of organic matter input in the sediment are also evident from the sediment $\delta^{13}C$ isotopic

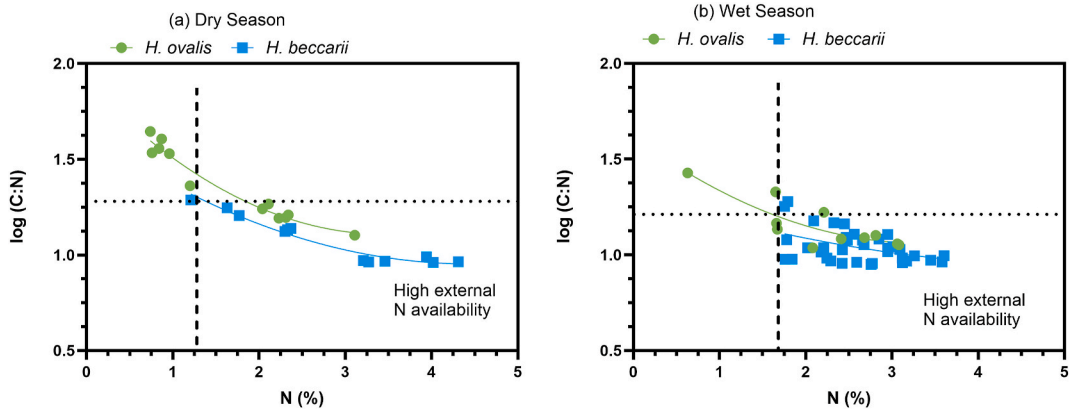

Fig. 5. Log (Y) transformed carbon to nitrogen ratios (C:N) versus nitrogen content (N%) in total biomass of *H. ovalis* and *H. beccarii* between a) wet and b) dry seasons in Hong Kong. Dashed lines indicate the threshold values for C:N and nitrogen ratios in global seagrasses, related to the balance between external nitrogen supply and internal utilization by the plants [Duarte, 1990].

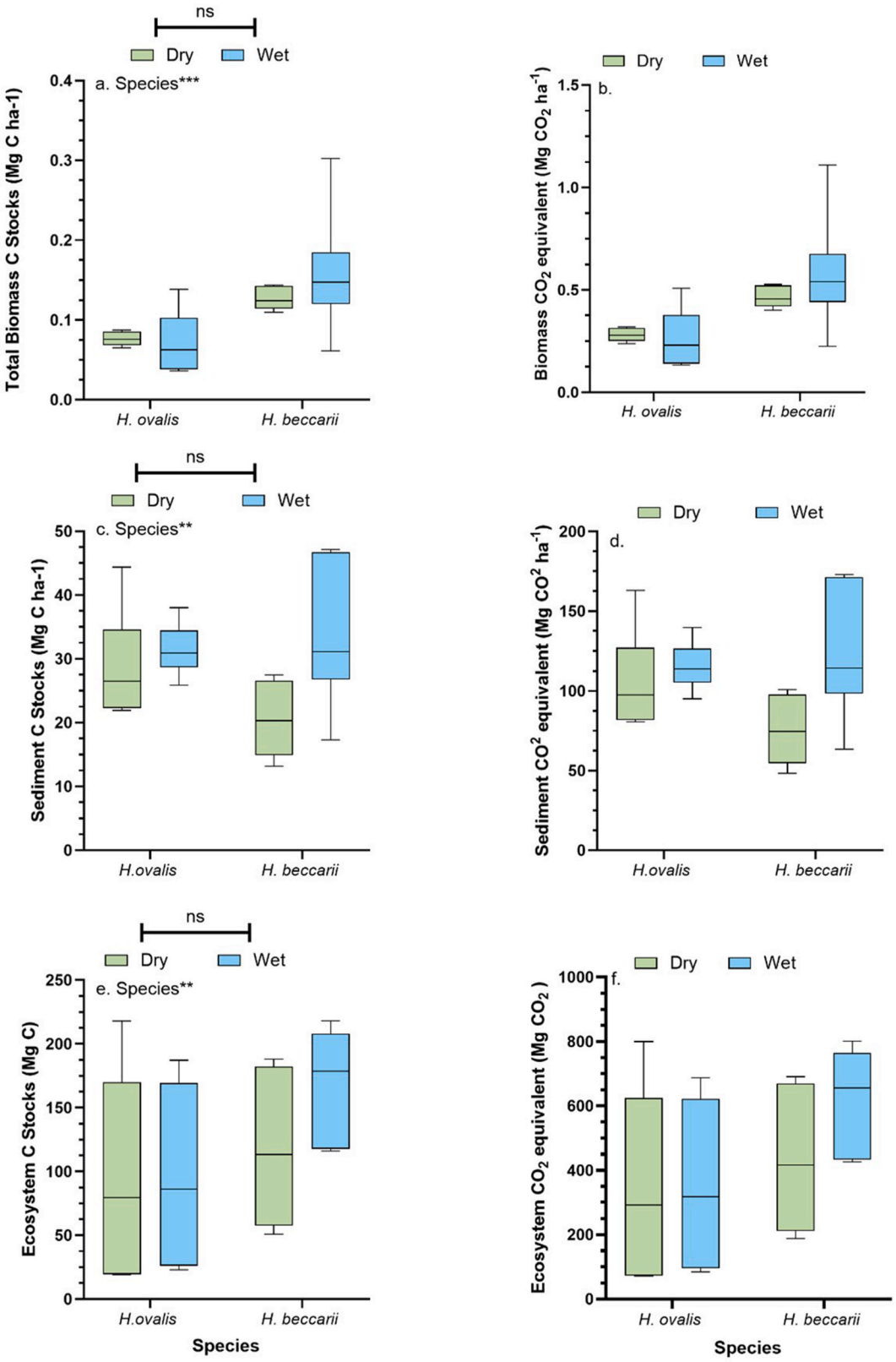

Fig. 6. Boxplot of seagrass biomass (aboveground + belowground; g DW m^{-2}) and sediment carbon stocks (Mg C ha^{-1}), against the respective CO_2 equivalent of *H. ovalis* and *H. beccarii* and associated sediment in dry and wet seasons in Hong Kong. Statistical significance ($p < 0.05$) was derived from a two-way ANOVA analysis using season (dry and wet), and species (*H. ovalis* and *H. beccarii*) as fixed factors ($p < 0.0001$***, $p < 0.001$**, $p < 0.05$*, not significant = ns). Statistical tests were not conducted for CO_2 equivalent (b, d and e).

signatures, suggesting increased presence of marine and freshwater particulate organic carbon and dissolved organic carbon sources during the wet season (Fig. 5). Furthermore, both seagrass species and their surrounding habitats are inhabited by other coastal vegetated habitats (i.e., mangroves and saltmarshes; Fig. S5) that could also have contributed towards the increase in sediment organic matter (Huang et al., 2015; Meng et al., 2019; Fu et al., 2020; Martins et al., 2022). The contribution of organic matter from adjacent saltmarshes and mangroves into *H. beccarii* meadows has been reported from similar intertidal mudflats in the Pearl Bay and Guangxi Bay areas of coastal China (Ren et al., 2024; Su et al., 2020) and for *H. ovalis* from Hainan Province, China (Du et al., 2019).

In general, seagrass species with a greater canopy height (i.e., longer leaf length) and a denser rhizome network can trap more sediment particles (Mazarrasa et al., 2018; Mishra and Apte, 2020; Mishra et al., 2021; Liu et al., 2020). The greater canopy height of *H. ovalis* may have aided organic matter accumulation in the wet season, compared to *H. beccarii*. Similarly, the dense rhizome network of *H. beccarii* helped in accumulation of 1.4-fold higher organic matter in the wet season than the dry season (Fig. 2a), which is evident from the 1.2-fold higher belowground biomass of *H. beccarii* than *H. ovalis* (Table S5). In addition to seagrass morphometric traits, the presence of macroalgae and *A. marina* root systems may have also promoted organic matter accumulation in *H. ovalis* meadows (Fig. S5). This increased accumulation of sediment particles and organic matter, together with the formation of muddy sediments (that reduce remineralization of C_{stocks}), may have supported the increased sediment C_{stocks} in both species in the wet season (Fig. 6; Table S4) (Mazarrasa et al., 2018; Miyajima et al., 2017). However, the reduction in seagrass biomass during the dry season (Table S5), and changes in local hydrodynamic conditions, can potentially promote the erosion of organic matter accumulated in the wet season and thus, the reduction of the sediment C_{stocks} (Egea et al., 2023b).

Seasonal variation in C_{stocks} composition (e.g., seagrass + algae) can also alter C_{stocks} accumulation at the sediment surface, thus affecting total sediment C_{stocks} (Zhang et al., 2022; Liu et al., 2016, 2022). In this study, seasonal variation in sediment C_{stocks} was evident for both species through increased sediment C_{stocks} content in the wet season, despite the sediment nitrogen content remaining comparable across seasons for both species (Fig. 5). During the wet season, the *H. ovalis*, meadows became overgrown with macroalgae (*Ulva* spp.), due to high nutrient availability (Table S5) (Su et al., 2020; Zhou et al., 2011), potentially providing a significant carbon source to the sediment carbon pool. However, this macroalgal carbon is highly labile, and could easily be remineralized if the organic matter is eroded due to the seagrass meadow becoming degraded or extirpated (Arina et al., 2023; Oreska et al., 2018). Although the contribution of macroalgae to the carbon was not explicitly measured, the sediment carbon content observed for *H. ovalis* in this study (1.24–1.36 %; Fig. 6c–Table S4) were comparable to carbon from Hainan Island, China [see 38], but were 8-fold higher than previous sediment carbon observed in Yongxing Island, China (0.31–0.32 %) (Jiang et al., 2019). Additionally, the range of *H. beccarii* sediment carbon observed in this study (0.80–1.33 %; Fig. 6c–Table S4) were also comparable to carbon found in other sites across China's coastline [see 69]. The differences in *H. ovalis* sediment carbon between our study and Yongxing Island are likely the result of limited riverine nutrient input, oligotrophic coastal waters and the presence of offshore carbonate sediments in *H. ovalis* meadows where organic matter content is lower, as described by Jiang et al. (2019).

Global studies have revealed that seagrass sediment $\delta^{13}C$ signatures contain carbon sources from multiple primary producers (i.e., mangroves, saltmarsh) (Kennedy et al., 2010). From this study, it is evident that sedimentary carbon sources of *H. ovalis* and *H. beccarii* exhibit seasonal differences (Fig. 4). The sediment and biomass $\delta^{13}C$ of both *H. ovalis* and *H. beccarii* observed in this study (+6.3 ± 0.2 ‰; Table S4, Table S5) are significantly lower than the global mean of $\delta^{13}C$ results reported for seagrass sediments globally (Kennedy et al., 2010). This suggests the sediment carbon composition in seagrass meadows in Hong Kong are composed of isotopically depleted carbon. In comparison, the sediment $\delta^{13}C$ data from this study falls within mean sediment $\delta^{13}C$ values (−24.9 ± 2.2 ‰; Table S4) reported for coastal vegetated ecosystems in China, confirming that the sediment C_{stocks} of seagrass meadows contain more terrestrial-derived allochthonous and marine-derived carbon, than carbon from seagrass plants (Fu et al., 2021). However, to confirm these conclusions about isotopic signals, further evaluation and additional data to perform isotopic model analyses are needed.

A key limitation in seagrass blue carbon research is the knowledge gap in species-specific C_{stocks} data, particularly for smaller seagrass species, constraining general inferences and C_{stocks} quantifications (Kennedy et al., 2022; Mishra et al., 2023; Ricart et al., 2020; Stankovic et al., 2023). This study addressed this limitation, finding significant species-specific differences in total biomass (aboveground + belowground) C_{stocks} in both *H. ovalis* (0.07–0.08 Mg C ha^{-1}) and *H. beccarii* (0.13–0.16 Mg C ha^{-1}; Table S5, Fig. S5). These C_{stocks} values are comparable to previous studies determining the total biomass of *H. beccarii* across China's coastline (Jiang et al., 2017a, 2017b; Ren et al., 2024). However, the biomass C_{stocks} observed for *H. ovalis* in this study were similar to *H. ovalis* biomass C_{stocks} from Qilianyu Lagoon, China (0.04–0.10 Mg C ha^{-1}), but lower than those from Hainan Island, China (0.20–0.28 Mg C ha^{-1}) (Jiang et al., 2017a, 2019). These contrasting findings are likely due to the differences in total biomass of *H. ovalis* (16.46–97.1 g DW $m^{-2}$and *H. beccarii* (31.41 g DW m^{-2}), as well as the biomass C_{stocks} (*H. ovalis*; 0.08–0.07 Mg C ha^{-1}, *H. beccarii*; 0.13–0.16 Mg C ha^{-1}; Table S5) (Jiang et al., 2017a, 2019).

The supply of nitrogen in seagrass ecosystems is typically limited, but high standing stocks of nitrogen can lead to higher growth rates (Papadimitriou et al., 2005). The Pearl River is affected by highly seasonal, anthropogenic nitrogen loading (Archana et al., 2018) resulting in higher $\delta^{15}N$ values in both seagrass species during the wet season (Fig. 5). Seagrass biomass C:N ratios are good indicators of a higher nitrogen assimilation rate (Duarte, 1990; Lee and Dunton, 2000), with higher C:N ratios and lower nitrogen levels evident for *H. ovalis* in the dry season, where lower relative nitrogen assimilation occurred (Fig. 5). This increased nutrient enrichment during the wet season likely facilitated *H. beccarii* meadows in generating ~1.5-fold higher aboveground and belowground biomass, with enriched $\delta^{15}N$ (5.9–12.20 ‰; Table S5) accumulation in belowground tissues, in comparison to the dry season (Table S5). Such enriched $\delta^{15}N$ values are also an indication of local wastewater input from raw sewage, which has been observed in coastal waters surrounding Hong Kong (Archana et al., 2018), and for *H. beccarii* meadows in regions of coastal China (Luo et al., 2022). Similarly, eutrophication has been observed to lead to higher $\delta^{15}N$ values (9.3 ‰) in *H. ovalis* meadows across China's coastline (Lin et al., 2021).

Conversely, chronic nutrient enrichment can profoundly alter seagrass meadows over short-term and decadal timescales, leading to shifts in ecosystem structure and function (Liu et al., 2016, 2022). Elevated nutrient levels often lead to the proliferation of epiphytes and macroalgae, which outcompete seagrasses (Liu et al., 2022). Nutrient-loaded seagrass litter also reduces leaf litter quality (i.e., low in recalcitrant organic matter concentrations), which can inhibit long-term carbon sequestration in seagrass meadows (Liu et al., 2024). Over time, chronic nutrient enrichment can disrupt multiple seagrass biochemical pathways and microbial activity, resulting in lower seagrass biomass and reduced contribution of seagrass to long-term C_{stocks} (Liu et al., 2016, 2022); which has been reported in populations for both *H. ovalis* and *H. beccarii* across China (Zhang et al., 2022; Yang et al., 2018; Jiang et al., 2022; Liu et al., 2024).

From this study, it is evident that in smaller seagrass species such as *H. ovalis* and *H. beccarii,* total C_{stocks} (biomass + sediment) are dominated by sediment C_{stocks} (99 %) rather than biomass (Fig. 6c–Table S4, Table S5). The range of total C_{stocks} in *H. ovalis* (28.97–31.54 Mg C ha^{-1})

and *H. beccarii* (20.64–34.01 Mg C ha^{-1}) sediment showed the greatest fluctuations in relation to seasonal nutrient input, in comparison to minimal changes in biomass C_{stocks} (Fig. 6a–Table S4, Table S5). Though the contribution of biomass carbon towards total C_{stocks} seems minimal, it is important to note that sedimentary carbon burial in part originated from the degradation of seagrass plant material, therefore highlighting the key contributory role of sediment C_{stocks}. In addition, these small seagrass species also support significant biogeochemical functions (e.g., trapping sediment particles from the water column in rhizome networks, burial and cycling of autochthonous carbon), which also provide major contributions towards sediment C_{stocks} (Ren et al., 2024; Su et al., 2020; Wu et al., 2020; Zou et al., 2021). Consequently, the belowground biomass of both seagrass species contributed significantly towards the sediment C_{stocks} pool, especially in the wet season, when growth is higher (Fig. 4, Table S5).

A recent review (Macreadie et al., 2021) estimated that management of blue carbon ecosystems (inc. Seagrasses, mangroves, saltmarshes etc.) could mitigate ~3 % of annual global greenhouse gas emissions. However, the significant C_{stocks} found in this study in the upper sedimentary layer (15 cm) of the two seagrass species studied, compared to other areas of China, highlight their potential to be utilized as a NbS to climate change mitigation and contribute towards Hong Kong's Climate Action Plan 2050 (Hong Kong SAR Government, 2021). Further, the total CO_2 accumulation capacity of Hong Kong's seagrass meadows across seasons (780.37–972.61 Mg CO_2) are presently incongruous with national climate action plans (i.e., reduction ~20 billion tons by 2030) (Hong Kong SAR Government, 2021). It should be noted that: i) estimates were based on the upper sedimentary layer (15 cm), and ii) the meadows surveyed represent only 16.41 ha of Hong Kong's total coastal area (~164,000 ha). Further interannual assessments of total C_{stocks} for the entire extent of Hong Kong's seagrass meadows are essential to comprehensively determine the blue carbon potential of seagrass ecosystems for Hong Kong. The C_{stocks} storage potential of these seagrasses have important implications for carbon accounting in Hong Kong, underscoring the need for urgent management action of these rapidly declining seagrass populations, and other coastal wetland ecosystems, at both local and regional scales.

5. Conclusions

This study, for the first time, elucidates seasonal changes in C_{stocks} in seagrass biomass and sediment for the dominant seagrass species in Hong Kong, addressing important geographical, species-specific and seasonal knowledge gaps in seagrass blue carbon research across Southeast Asia and the coast of China. Although the results presented here represent a fraction of the total coastline in the Greater Bay Area (i.e., Guangdong, Hong Kong and Macao), this study provides insights into how seasonality and local nutrient loading (a proxy of urbanization) are driving changes in seagrass blue carbon stocks. Additionally, this study provides important baseline data of C_{stocks} in *H. ovalis* and *H. beccarii* meadows, which are prone to local nutrient loading from anthropogenic and riverine inputs, and how these impacts alter seagrass biomass and sediment carbon storage.

CRediT authorship contribution statement

Amrit Kumar Mishra: Writing – review & editing, Writing – original draft, Visualization, Methodology, Investigation, Formal analysis, Data curation. **Katie M. Watson:** Writing – review & editing, Visualization, Validation, Methodology, Data curation. **Ho Tun Ng:** Writing – review & editing, Methodology, Investigation. **Man Zhao:** Writing – review & editing, Visualization, Validation, Methodology, Investigation. **Chanaka Isuranga Premarathne Maha Ranvilage:** Writing – review & editing, Methodology, Investigation. **Dwi Wai Shan Jaimie:** Writing – review & editing, Methodology, Investigation. **Tse Cham Man:** Writing – review & editing, Methodology, Investigation. **Christelle Not:** Writing – review & editing, Validation, Resources, Methodology, Investigation. **Benoit Thibodeau:** Writing – review & editing, Validation, Resources, Methodology, Investigation. **Juan C. Astudillo:** Writing – review & editing, Validation, Software, Resources, Methodology. **Juan Diego Gaitán-Espitia:** Writing – review & editing, Writing – original draft, Validation, Supervision, Resources, Project administration, Methodology, Investigation, Funding acquisition, Formal analysis, Data curation, Conceptualization.

Data availability statement

All data is available at: Watson, Katie Margaret (2025). DATA repository for: Seasonality and local nutrient loading drive changes in organic carbon in seagrass ecosystems in Hong Kong. HKU Data Repository. Dataset. https://doi.org/10.25442/hku.28693532.v1.

Declaration of competing interest

The authors declare that they have no known competing financial interests or personal relationships that could have appeared to influence the work reported in this paper.

Acknowledgements

This project was supported by the Hong Kong Marine Conservation and Enhancement Fund (MCEF20001). JDGE was supported by the AFCD Environmental Conservation Fund (Project No. 107/2022) and the Faculty of Science RAE Improvement Fund 2022–2023, The University of Hong Kong. BT was partially supported by a Research Grants Council grant from the Hong Kong SAR, China (Project Reference Number: AoE/P-601/23-N). We are thankful to Chik Hei Yeung for support in fieldwork and laboratory sample analysis, and to Leung Kit Sum for assistance with stable isotope processing.

Appendix A. Supplementary data

Supplementary data to this article can be found online at https://doi.org/10.1016/j.ecss.2025.109427.

References

Adams, M.P., et al., 2020. Predicting seagrass decline due to cumulative stressors. Environ. Model. Software 130, 104717.
Alongi, D.M., 2020. Carbon balance in salt marsh and mangrove ecosystems: a global synthesis. J. Mar. Sci. Eng. 8, 767.
Archana, A., et al., 2018. Nitrogen sources and cycling revealed by dual isotopes of nitrate in a complex urbanized environment. Water. Res. 142, 459–470.
Arina, N., et al., 2023. Algal contribution to organic carbon sequestration and its signatures in a tropical seagrass meadow. Deep-Sea Res. II: Top. Stud. Oceanogr. 210, 105307.
Barcelona, A., Oldham, C., Colomer, J., Garcia-Orellana, J., Serra, T., 2021. Particle capture by seagrass canopies under an oscillatory flow. Coast. Eng. 169, 103972.
Bass, A.V., Falkenberg, L.J., 2023. Two tropical seagrass species show differing indicators of resistance to a marine heatwave. Ecol. Evol. 13, e10304.
Burkholder, J.M., Tomasko, D.A., Touchette, B.W., 2007. Seagrasses and eutrophication. J. Exp. Mar. Biol. Ecol. 350, 46–72.
Chausson, A., et al., 2020. Mapping the effectiveness of nature-based solutions for climate change adaptation. Glob. Change Biol. 26, 6134–6155.
Chen, Z.L., Lee, S.Y., 2022. Sediment carbon sequestration and sources in peri-urban tidal flats and adjacent wetlands in a megacity. Mar. Pollut. Bull. 185, 114368.
Christianson, A.B., et al., 2022. The promise of blue carbon climate solutions: where the science supports ocean-climate policy. Front. Mar. Sci. 9, 851448.
Cressie, N., 1988. A graphical procedure for determining nonstationarity in time series. J. Am. Stat. Assoc. 83 (404), 1108–1116.
Dahl, M., et al., 2020. High seasonal variability in sediment carbon stocks of cold-temperate seagrass meadows. J. Geophys. Res-Biogeo. 125 (1), e2019JG005430.
Dencer-Brown, A.M., et al., 2022. Integrating blue: how do we make nationally determined contributions work for both blue carbon and local coastal communities? Ambio 51, 1978–1993.
do Amaral Camara Lima, M., et al., 2023. A review of seagrass ecosystem services: providing nature-based solutions for a changing world. Hydrobiologia 850, 2655–2670.

Du, J., et al., 2019. Analysis of organic carbon sources in tropical seagrass fish: a case study of the east coast of Hainan province. Mar. Biol. Res. 15, 513–522.
Duarte, C.M., 1990. Seagrass nutrient content. Mar. Ecol. Prog. Ser. 67, 201–207.
Duarte de Paula Costa, M., Macreadie, P.I., 2022. The evolution of blue carbon science. Wetlands 42, 109.
Egea, L.G., Jiménez-Ramos, R., Hernández, I., Brun, F.G., 2020. Differential effects of nutrient enrichment on carbon metabolism and dissolved organic carbon (DOC) fluxes in macrophytic benthic communities. Mar. Environ. Res. 162, 105179.
Egea, L.G., et al., 2023a. Effect of marine heat waves on carbon metabolism, optical characterization, and bioavailability of dissolved organic carbon in coastal vegetated communities. Limnol. Oceanogr. 68, 467–482.
Egea, L.G., Infantes, E., Jiménez-Ramos, R., 2023b. Loss of POC and DOC on seagrass sediments by hydrodynamics. Sci. Total Environ. 901, 165976.
Environmental Protection Department, 2024. Marine water quality data. Environmental Protection Interactive. *Centre*. https://cd.epic.epd.gov.hk/EPICRIVER/marine/.
Fong, C., 1998. Some Aspects of the Ecology of the Seagrass *Zostera japonica* in Hong Kong (Thesis). University of Hong Kong, Hong Kong SAR. https://doi.org/10.5353/th_b3122079. Retrieved from.
Fu, C., et al., 2020. Stocks and losses of soil organic carbon from Chinese vegetated coastal habitats. Glob. Chang. Biol. 27, 202–214.
Fu, C., et al., 2021. Stocks and losses of soil organic carbon from Chinese vegetated coastal habitats. Glob. Change Biol. 27 (1), 202–214.
Gao, G., et al., 2022. A review of existing and potential blue carbon contributions to climate change mitigation in the anthropocene. J. Appl. Ecol. 59, 1686–1699.
Gu, Y.G., et al., 2012. Multivariate statistical and GIS-based approach to identify source of anthropogenic impacts on metallic elements in sediments from the mid Guangdong coasts, China. Environ. Pollut. 163, 248–255.
Hong Kong SAR Government, 2021. Hong Kong's climate action plan 2025. Carbon Neutral@HK. https://www.eeb.gov.hk/sites/default/files/pdf/cap_2050_en.pdf.
Coastal blue carbon: methods for assessing carbon stocks and emissions factors in mangroves, tidal salt marshes, and seagrasses. In: Howard, J., Hoyt, S., Isensee, K., Telszewski, M., Pidgeon, E. (Eds.), 2014. Conservation International, Intergovernmental Oceanographic Commission of UNESCO. International Union for Conservation of Nature, Arlington, Virginia, USA.
Huang, Y.H., Lee, C.L., Chung, C.Y., Hsiao, S.C., Lin, H.J., 2015. Carbon budgets of multispecies seagrass beds at Dongsha Island in the South China Sea. Mar. Environ. Res. 106, 92–102.
Jiang, Z., et al., 2017a. Newly discovered seagrass beds and their potential for blue carbon in the coastal seas of Hainan Island, South China Sea. Mar. Pollut. Bull. 125, 513–521.
Jiang, Z., et al., 2017b. Newly discovered seagrass beds and their potential for blue carbon in the coastal seas of Hainan Island, South China Sea. Mar. Pollut. Bull. 125 (1–2), 513–521.
Jiang, Z., et al., 2019. Contrasting root length, nutrient content and carbon sequestration of seagrass growing in offshore carbonate and onshore terrigenous sediments in the South China Sea. Sci. Total Environ. 662, 151–159.
Jiang, Z., et al., 2020. Historical changes in seagrass beds in a rapidly urbanizing area of Guangdong province: implications for conservation and management. Glob. Ecol. Conserv. 22, e01035.
Jiang, Z., et al., 2022. Eutrophication reduced the release of dissolved organic carbon from tropical seagrass roots through exudation and decomposition. Mar. Environ. Res. 179, 105703.
Johannessen, S.C., 2022. How can blue carbon burial in seagrass meadows increase long-term, net sequestration of carbon? A critical review. Environ. Res. Lett. 17, 093004.
Kennedy, H., et al., 2010. Seagrass sediments as a global carbon sink: isotopic constraints. Global Biogeochem. Cycles 24, GB4026.
Kennedy, H., Pagès, J.F., Lagomasino, D., Colarusso, P., Fourqurean, J.W., 2022. Species traits and geomorphic setting as drivers of global soil carbon stocks in seagrass meadows. Global Biogeochem. Cycles 36, e2022GB007481.
Lee, K.S., Dunton, K.H., 2000. Effects of nitrogen enrichment on biomass allocation, growth, and leaf morphology of the seagrass *Thalassia testudinum*. Mar. Ecol. Prog. Ser. 196, 39–48.
Lin, J., et al., 2021. Trophic importance of the seagrass *Halophila ovalis* in the food web of a Hepu seagrass bed and adjacent waters, Beihai, China. Ecol. Indic. 125, 107607.
Liu, S., et al., 2016. Effect of nutrient enrichment on the source and composition of sediment organic carbon in tropical seagrass beds in the South China Sea. Mar. Pollut. Bull. 110, 274–280.
Liu, S., et al., 2020. Nutrient loading diminishes the dissolved organic carbon drawdown capacity of seagrass ecosystems. Sci. Total Environ. 740, 140185.
Liu, S., et al., 2022. Nutrient loading decreases blue carbon by mediating fungi activities within seagrass meadows. Environ. Res. 212, 113280.
Liu, S., et al., 2024. Nutrient-loaded seagrass litter experiences accelerated recalcitrant organic matter decay. Sci. Total Environ. 953, 176251.
Luo, H., et al., 2022. Eutrophication decreases *Halophila beccarii* plant organic carbon contribution to sequestration potential. Front. Mar. Sci. 9, 986415.
Macreadie, P.I., et al., 2019. The future of blue carbon science. Nat. Commun. 10 (1), 3998.
Macreadie, P.I., et al., 2021. Blue carbon as a natural climate solution. Nat. Rev. Earth Environ. 2, 826–839.
Martins, M., et al., 2022. Carbon and nitrogen stocks and burial rates in intertidal vegetated habitats of a mesotidal coastal lagoon. Ecosyst 25, 372–386.
Mazarrasa, I., et al., 2018. Habitat characteristics provide insights of carbon storage in seagrass meadows. Mar. Pollut. Bull. 134, 106–117.
Meng, W., Feagin, R.A., Hu, B., He, M., Li, H., 2019. The spatial distribution of blue carbon in the coastal wetlands of China. Estuar. Coast. Shelf. Sci. 222, 13–20.
Mishra, A., Apte, D., 2020. Ecological connectivity with mangroves influences tropical seagrass population longevity and meadow traits within an island ecosystem. Mar. Ecol. Prog. Ser. 644, 47–63.
Mishra, A.K., Khadanga, M.K., Patro, S., Apte, D., Farooq, S.H., 2021. Population structure of a newly recorded (*Halodule uninervis*) and native seagrass (*Halophila ovalis*) species from an intertidal creek ecosystem. Lake Reserv.: Sci. Policy Manag. Sustain. Use 26, e12376.
Mishra, A.K., Acharya, P., Apte, D., Farooq, S.H., 2023. Seagrass ecosystem adjacent to mangroves store higher amount of organic carbon of Andaman and Nicobar Islands, Andaman Sea. Mar. Pollut. Bull. 193, 115135.
Miyajima, T., et al., 2017. Geophysical constraints for organic carbon sequestration capacity of *Zostera marina* seagrass meadows and surrounding habitats. Limnol. Oceanogr. 62 (3), 954–972.
Morton, B., 2016. Hong Kong's mangrove biodiversity and its conservation within the context of a southern Chinese megalopolis. A review and a proposal for Lai Chi Wo to be designated as a world heritage site. Reg. Stud. Mar. Sci. 8, 382–399.
Nordhaus, W.D., 2017. Revisiting the social cost of carbon. Proc. Natl. Acad. Sci. USA. 114, 1518–1523.
Nordlund, L.M., Koch, E.W., Barbier, E.B., Creed, J.C., 2016. Seagrass ecosystem services and their variability across genera and geographical regions. PLoS One 11, e0163091.
Oreska, M.P.J., et al., 2018. Non-seagrass carbon contributions to seagrass sediment blue carbon. Limnol. Oceanogr. 63 (S1), S3–S18.
Papadimitriou, S., Kennedy, H., Kennedy, D.P., Borum, J., 2005. Seasonal and spatial variation in the organic carbon and nitrogen concentration and their stable isotopic composition in *Zostera marina* (Denmark). Limnol. Oceanogr. 50, 1084–1095.
Pazzaglia, J., et al., 2020. Does warming enhance the effects of eutrophication in the seagrass *posidonia Oceanica*? Front. Mar. Sci. 7, 564805.
Phillips, D.L., Gregg, J.W., 2003. Source partitioning using stable isotopes: coping with too many sources. Oecologia 136, 261–269.
Phillips, D.L., Newsome, S.D., Gregg, J.W., 2005. Combining sources in stable isotope mixing models: alternative methods. Oecologia 144, 520–527.
Premarathne, C., et al., 2021. Low light availability reduces the subsurface sediment carbon content in *Halophila beccarii* from the South China Sea. Front. Plant Sci. 12, 664060.
Rahayu, Y.P., et al., 2023. Sedimentary seagrass carbon stock and sources of organic carbon across contrasting seagrass meadows in Indonesia. Environ. Sci. Pollut. Res. 30, 97754–97764.
Ren, Y., et al., 2024. Seagrass decline weakens sediment organic carbon stability. Sci. Total Environ. 937, 173523.
Ricart, A.M., York, P.H., Bryant, C.V., Rasheed, M.A., 2020. High variability of blue carbon storage in seagrass meadows at the estuary scale. Sci. Rep. 10, 5865.
Ricke, K., Drouet, L., Caldeira, K., Tavoni, M., 2018. Country-level social cost of carbon. Nat. Clim. Change 8, 895–900.
Sachithanandam, V., et al., 2022. Effect of hydrodynamic conditions on seagrass ecosystems during Cyclone Lehar in the South Andaman Islands, India. Ecohydrol. Hydrobiol. 22 (4), 640–659.
Salinas, C., et al., 2020. Seagrass losses since mid-20th century fuelled CO_2 emissions from soil carbon stocks. Glob. Change Biol. 26, 4772–4784.
Serrano, O., Lavery, P.S., Bongiovanni, J., Duarte, C.M., 2020. Impact of seagrass establishment, industrialization and coastal infrastructure on seagrass biogeochemical sinks. Mar. Environ. Res. 160, 104990.
Shi, Y., et al., 2010. Overview on seagrasses and related research in China. Chin. J. Oceanol. Limnol. 28, 329–339.
Soissons, L.M., et al., 2018. Latitudinal patterns in European seagrass carbon reserves: influence of seasonal fluctuations versus short-term stress and disturbance events. Front. Plant Sci. 9, 88.
Stankovic, M., et al., 2021. Quantification of blue carbon in seagrass ecosystems of Southeast Asia and their potential for climate change mitigation. Sci. Total Environ. 783, 146858.
Stankovic, M., et al., 2023. Blue carbon assessments of seagrass and mangrove ecosystems in South and Southeast Asia: current progress and knowledge gaps. Sci. Total Environ. 904, 166618.
Su, Z., Qiu, G., Fan, H., Li, M., Fang, C., 2020. Changes in carbon storage and macrobenthic communities in a mangrove-seagrass ecosystem after the invasion of smooth cordgrass in southern China. Mar. Pollut. Bull. 152, 110887.
Tanacredi, J.T., Botton, M.L., Smith, D.R. (Eds.), 2009. Biology and Conservation of Horseshoe Crabs, Biology and Conservation of Horseshoe Crabs. Springer, Boston, Maryland, USA.
Trevathan-Tackett, S.M., et al., 2015. Comparison of marine macrophytes for their contributions to blue carbon sequestration. Ecology 96, 3043–3057.
United Nations Environment Programme, 2020. Protecting Seagrass Through Payments for Ecosystem Services: a Community Guide. UNEP, Nairobi, Kenya.
Unsworth, R.K.F., et al., 2019. Global challenges for seagrass conservation. Ambio 48, 801–815.
Wang, Y., et al., 2021. Coastal eutrophication in China: trend, sources, and ecological effects. Harmful Algae 107, 102058.
Wang, X., Bai, J., Yan, J., Cui, B., Shao, D., 2022. How turbidity mediates the combined effects of nutrient enrichment and herbivory on seagrass ecosystems. Front. Mar. Sci. 9, 787041.
Ward, M.A., et al., 2021. Blue carbon stocks and exchanges along the California coast. Biogeosciences 18, 4717–4732.
Wu, J., et al., 2020. Opportunities for blue carbon strategies in China. Ocean Coast Manag. 194, 105241.

Xu, J., et al., 2008. Temporal and spatial variations in nutrient stoichiometry and regulation of phytoplankton biomass in Hong Kong waters: influence of the Pearl river outflow and sewage inputs. Mar. Pollut. Bull. 57 (6–12), 335–348.
Xuan, D.T.L., Phan, T.T.H., Hoang, C.T., Ton, T.P., Luong, Q.D., 2022. Growth and morphological responses of *Halophila beccarii* to low salinity. Hue. Univ. J. Sci. Nat. Sci. 131, 47–57.
Yamuza-Magdaleno, A., Jiménez-Ramos, R., Casal-Porras, I., Brun, F.G., Egea, L.G., 2024. Long-term sediment organic carbon remineralization in different seagrass and macroalgae habitats: implication for blue carbon storage. Front. Mar. Sci. 11, 1370768.
Yang, X., et al., 2018. Evaluation of four seagrass species as early warning indicators for nitrogen overloading: implications for eutrophic evaluation and ecosystem management. Sci. Total Environ. 635, 1132–1143.
Ye, F., Ni, Z., Xie, L., Wei, G., Jia, G., 2015. Isotopic evidence for the turnover of biological reactive nitrogen in the Pearl river Estuary, south China. J. Geophys. Res-Biogeo. 120, 661–672.
Zhang, Y.H., et al., 2020. Seagrass resilience: where and how to collect donor plants for the ecological restoration of eelgrass *Zostera marina* in Rongcheng Bay, Shandong Peninsula, China. Ecol. Eng. 158, 106029.
Zhang, X., et al., 2022. Nutrient enrichment decreases dissolved organic carbon sequestration potential of tropical seagrass meadows by mediating bacterial activity. Ecol. Indic. 145, 109576.
Zhou, W., et al., 2011. Bacterioplankton dynamics along the gradient from highly eutrophic Pearl river Estuary to oligotrophic northern South China Sea in wet season: implication for anthropogenic inputs. Mar. Pollut. Bull. 62 (4), 726–733.
Zou, Y.F., Chen, K.Y., Lin, H.J., 2021. Significance of belowground production to the long-term carbon sequestration of intertidal seagrass beds. Sci. Total Environ. 800, 149579.
Zribi, I., et al., 2023. Effect of shading imposed by the algae *chaeotomorpha linum* loads on structure, morphology and physiology of the seagrass *Cymodocea nodosa*. Mar. Environ. Res. 188, 106001.